Dynamics of an Anchored Polymer Molecule under an Oscillating Force

A. K. Chattopadhyay[1] and D. Marenduzzo[2]

[1]*Dipartimento di Fisica "G. Galilei," Universitá degli Studi di Padova, via Marzolo 8, 35131 Padova, Italy*
[2]*SUPA, School of Physics, University of Edinburgh, Edinburgh EH9 3JZ, United Kingdom*

(Received 31 January 2006; revised manuscript received 21 September 2006; published 20 February 2007)

We study the dynamics of a polymer of varying stiffness, pinned or grafted at both ends and subjected to an oscillatory forcing at an intermediate point. Via stochastic simulations, we find a crossover from a periodic limit cycle to an aperiodic dynamics as the polymer gets "stiffer." An analytical argument valid in the 2D grafted case shows that in such a case this aperiodic dynamics has some chaotic signatures.

DOI: 10.1103/PhysRevLett.98.088101 PACS numbers: 87.15.La, 36.20.Ey, 64.60.Ht, 87.15.He

Recent times have witnessed an outburst in the development and use of single molecule techniques [1,2]. It is now possible to study a single molecule with atomic force microscopes (AFMs), laser tweezers, etc., and to apply a local force of a prescribed shape ideally at any section of the polymer under scrutiny. While these experiments are of interest *per se*, as they allow precise measurements of elastic properties of bio- and artificial polymers, they may also shed light on some *in vivo* situations in which cellular machineries or protein complexes exert a localized force on segments of a biopolymer. A popular example of this is found in DNA unzipping during replication, in which helicases bind at the two ends of an "eye" (or replication bubble) and unwind the DNA locally [3,4]. Other suggestive examples involve DNA transcription, when RNA polymerases may apply a force to reel in and transcribe a gene [5], or in cytoskeletal dynamics, as motor proteins continuously push and pull actin fibers and microtubules [3].

Barring notable exceptions [6,7], theory and experiments have most often focused on equilibrium descriptions. While this is important, there still remain many interesting but as yet unanswered questions on the dynamics of a single polymer [8].

Here we suggest a possible setup for a single molecule experiment where we consider a polymer of variable stiffness anchored at both ends and subjected to a periodic force at an interior point. By monitoring the 3D time evolution of the polymer chunk under tension via dynamic Monte Carlo simulations, we predict a crossover from a periodic limit cycle in the position-force plane, observed for very flexible chains, to an aperiodic behavior for stiffer polymers. The shape of this orbit depends on the magnitude and periodicity of the forcing. An analytical treatment of the 2D polymer model grafted at one end, and using the mapping used in Ref. [9], shows that this system, in the semiflexible regime, could have a deterministic analogue with a positive Lyapunov exponent. The different dynamical states we predict may be checked via single molecule experiments in which the point of application of the force can be controlled. This would yield time series of the data analogous to the ones we compute. The polymer needs to be perturbed with a frequency larger than or comparable to its inverse relaxation time to observe the phenomena we predict. Ideal candidate systems to verify our predictions might thus be long dsDNA molecules or actin or amyloid fibers (whose relaxation times ranges from milliseconds to seconds; see the discussion at the end) [1].

We first consider the full 3-dimensional dynamics of a (strictly inextensible) semiflexible and self-avoiding polymer (of variable stiffness) subject to a time-dependent force $\vec{f}(t)$ applied at the jth bead of the chain, which is at $\vec{r}_j$, with $j = sN$, $0 < s < 1$ (the chain is constituted by N beads of diameter a joined by $N - 1$ links of length a—in what follows, simulation length scales are measured in units of a). We follow the time evolution of the polymer via 3-dimensional dynamic Monte Carlo simulations involving the kink-jump algorithm [10]. One Monte Carlo step (MCS) corresponds to a series of N attempted kink-jump moves. This method has recently been successfully

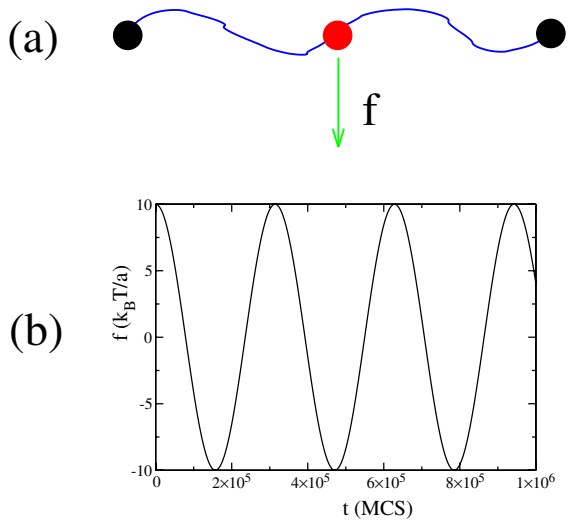

FIG. 1 (color online). Setup of our calculation. A semiflexible chain pinned at both ends and acted upon by an oscillating force (a) applied at its midpoint or (b) at a generic point between its extremities.

used in a number of contexts [11,12]. It allows only an indirect mapping to physical times, and it disregards hydrodynamic interactions between beads, but it is useful here as it allows an exact handling of the inextensibility constraint, as there is no need to introduce soft springs between monomers. The Hamiltonian $\mathcal{H}$ describing the single molecule setup in which we are interested is $\mathcal{H} = K_b \sum_{i=1}^{N-2} \vec{t}_i \cdot \vec{t}_{i+1} + \vec{f}(t) \cdot \vec{r}_{sN}$, where $K_b \equiv L_p k_B T$ is the bending rigidity (L_p, k_B, and T are, respectively, the persistence length, Boltzmann constant, and temperature) and $\vec{t}_i$ denotes the ith link ($1 \leq i < N$). Results are reported primarily for pinned boundary conditions. This means that the first and last beads are constrained to stay at $(0, 0, 0)$ and $(d, 0, 0)$, with $d < L \equiv Na$. For selected cases, we considered polymers grafted at (i) one end ($i = 1$) and (ii) both ends. In these cases, the first and last links were constrained to lie along the x direction as well. Typical values for other parameters were $L = 100a$, $d/L = 0.6$, and L_p/L between 0 and 0.2 (results are similar for smaller d/L). The periodic force along the z direction is $\vec{f}(t) = \hat{z}A\cos(2\pi\omega t)$, where A is the amplitude of the perturbation (typically 10 $k_B T/a$) and $\omega \equiv 1/\tau$ its inverse period. Figure 1 shows the setup.

In what follows, time is measured in MCSs. To relate these observations to physical quantities, we will also report estimates for the polymer relaxation time τ_r. Note that the 3D MC algorithm we use works at a fixed temperature T, implying that, e.g., bead diffusion and friction cannot be inputted and should be calculated *a posteriori*.

Figures 2 and 3 show the dynamic trajectories in the $z_{L/2}(t) \equiv z(t)$, $f(t)$ plane for a flexible (Fig. 2, variable ω) and a semiflexible (Fig. 3, L_p/L from 0 to 0.1) polymer, respectively. The flexible polymer parameters may be mapped onto those of a polyethylene molecule of thickness $\sim$0.5 nm and contour length 50 nm, while the semiflexible polymer with $L_p/L = 0.1$ may represent, e.g., a 0.5 μm long DNA in a 0.1 M NaCl solution (close to physiological concentration), for which its effective thickness is 5 nm [13].

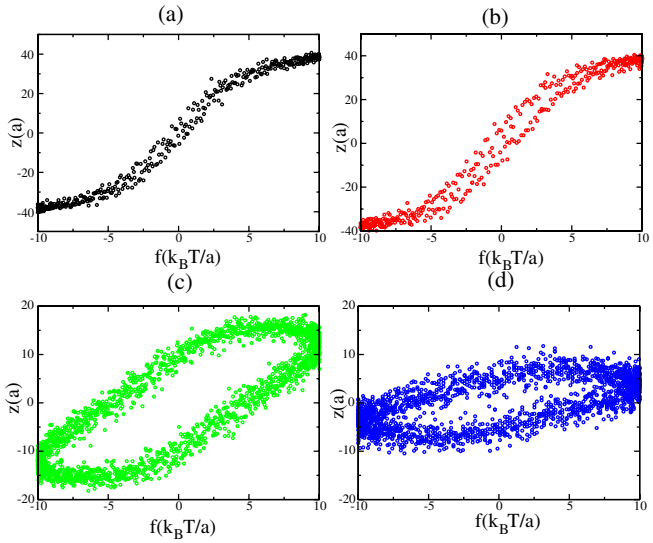

FIG. 2 (color online). Plot of $[(z(t), f(t)]$ for a flexible polymer with $1/2\pi\omega$ equal to (a) 20 000, (b) 1000, (c) 500, and (d) 250 (in MCSs). $\tau_r \sim 2500$ MCSs. $z(t)$ and $f(t)$ are in units of a and $k_B T/a$, respectively.

We begin with the flexible case. At quasiequilibrium, the dynamic trajectory of the point of application of a force $f(t)$ on a polymer along z ($\omega \to 0$) gives a 1D curve defined by $z(t) = \frac{\partial \log[\mathcal{Z}(\beta f, d)]}{\partial \beta f}$, where $\mathcal{Z}$ is the partition function of the system (which depends on d). Figure 2(a) shows that for $\tau \gg \tau_r$ the quasiequilibrium state is recovered. In Fig. 2, nonequilibrium effects creep in and the quasiequilibrium line is substituted by a hysteresis [Fig. 2(b)] or a limit cycle [Fig. 2(c)]. This crossover is due to the fact that the chain can no longer equilibrate at all times during the force ramping cycle, as now $\tau \sim \tau_r$. Thus, the midpoint position is sampled only on a portion of the phase space, which yields an under- (over)estimate of its value in the forward (backward) force scan; hence, hysteresis shows up. If ω is further increased [Fig. 2(d)], the trajectory followed by the limit cycle tilts toward the f axis.

The crossover between quasiequilibrium and limit cycle behavior could be observed in a flexible polymer with $L \gg L_p$. (Suitable candidates for an experiment would be long dsDNA's, with $L = 50$ μm or more, hence essentially flexible polymers with $\tau_r > 1$ s.) A stiffer polymer, such as a relatively short dsDNA or an actin fiber, enhances the

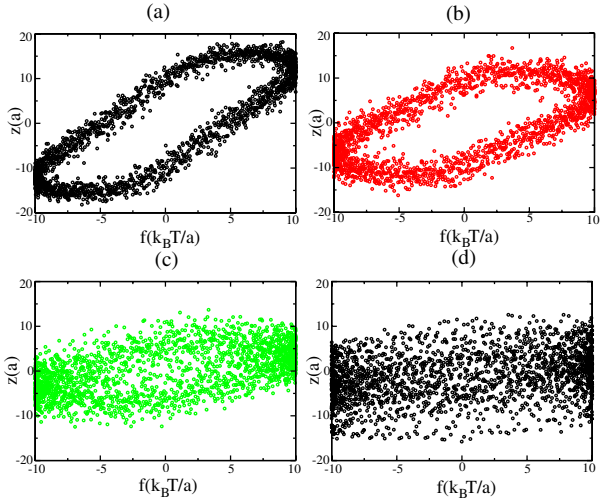

FIG. 3 (color online). $z(t)$ vs $f(t)$ for a polymer with $L = 100a$, $d/L = 0.6$, and variable L_p [respectively, (a) $L_p/L = 0$, (b) $L_p/L = 0.02$, (c) $L_p/L = 0.05$, and (d) $L_p/L = 0.1$]. x is the time-dependent position of the midpoint (at $s = L/2$). $c\tau \sim 3150$ MCSs while $\tau_r =$ (a) 2500, (b) 13 500, (c) 67 500, and (d) 110 000 (in MCSs [20]). $z(t)$ and $f(t)$ are in units of a and $k_B T/a$, respectively (for DNA in 0.1 M Na+ solution, $z = 5$ nm and $f = 0.8$ pN).

hysteresis. Under such circumstances, we no longer observe a (noisy) limit cycle, but the trajectories, representing the motion of the polymer midpoint, now fill the space in the (z, f) plane.

Figure 3 shows the crossover between these two different regimes. The limit cycle behavior typical of the flexible chain changes over to space filling trajectories for stiffer semiflexible polymers as we increase L_p/L. This space filling trajectory can be thought of as the superposition of several limit cycles, each of which spans only a limited range in z during a force cycle (forward and backward scan). This crossover resembles what happens in a Poincaré section in systems crossing over from a limit cycle behavior to chaotic dynamics (see, e.g., [14]). As time progresses, the instantaneous limit cycle at the midpoint is visiting drifts (along the z axis in Fig. 3), and this leads to the aperiodicity.

To assess the robustness of our results, we performed calculations with different boundary conditions, namely, with polymers grafted at one or both ends. In all cases, a crossover was found upon increasing L_p at a fixed L. The crossover value L_p^*/L is smaller with grafted boundary conditions (it is "easier" to get into the aperiodic regime there), while it only weakly depends on chain length over the values considered ($50a < L < 200a$ for pinned boundary conditions). We have attempted to qualitatively estimate the effect of hydrodynamic interactions, by performing simulations of the same system described by the potential in Eq. (1) with the stochastic rotation model [15] (this requires the introduction of soft nonlinear springs between monomers). While the crossover between a limit cycle to an aperiodic regime is still observed, our simulations suggest that the crossover occurs for larger L_p and ω than in the 3D MC simulations (the aperiodic zone in the dynamic phase diagram shrinks due to hydrodynamics). Details will be presented elsewhere.

To further characterize the aperiodic dynamic regime observed in a semiflexible polymer, it is instructive to compare our simulations with a semianalytical treatment. Toward this aim, we focus on a restricted 2D analysis of a semiflexible polymer grafted along the x direction and subjected to an oscillating transverse force at its end along z. Indeed, in 3D, our simulations *show* identical physics for grafted chains as in Ref. [16]. For a more rigorous theory, we resort to the theoretical technique reported in Ref. [9] and derive the Lyapunov exponent λ associated with the dynamics of 2D grafted polymers. We show that λ could be positive, implying that the observed aperiodic dynamics might have some chaotic signatures.

On general grounds, we may write the following equation for the coarse-grained tip dynamics:

$$\dot{z}(t) = -\Gamma \frac{\delta}{\delta z(t)}[k_B T \log P(z)] + f(t) + \eta(t), \quad (1)$$

$$P(z) = \frac{L_p\sqrt{3}}{\pi L^2}\int_{\infty}^{\infty} d\theta \exp\left\{-\frac{L_p\theta^2}{2L}\right\} \times \exp\left\{-\frac{6L_p[z - \sin\theta L]^2}{L^3}\right\}, \quad (2)$$

where δ denotes a functional derivative, the form of the transverse tip probability distribution $P(z)$ [whose logarithm defines $-\mathcal{F}(z)/k_BT$, $\mathcal{F}(z)$ being the free energy which governs the tip dynamics] is borrowed from Ref. [16], Γ is a suitable relaxation time, and η is a random noise whose 2-point correlation is $\langle \eta(t)\eta(t')\rangle = 2\Delta\delta(t - t')$ ($\Delta > 0$ gives the strength of noise, which we do not assume is fixed by the fluctuation-dissipation theorem as the system may be out of equilibrium, as in the simulations in Figs. 2 and 3). We set $\Gamma = 1$, which is tantamount to a rescaling of time.

The dynamics originating from Eq. (1) can be studied with the methods of Ref. [9] which lead to the following estimate for the largest λ of the dynamical system equivalent to ours (we assume that there exists one):

$$\lambda = \frac{1}{2}\int d\tau' \langle \zeta(\tau')\zeta(\tau + \tau')\rangle \cos 2\omega\tau', \quad (3)$$

where we have defined $\zeta(t) = \mathcal{F}''(z)$ [9].

For an exact evaluation of the Lyapunov exponent, we need a numerical solution for the tip dynamics as per Eq. (1). However, it is instructive to find an approximate semianalytical estimate. To this end, we evaluate $\mathcal{F}(z)$ and fit it to the two-state function $f(z) \equiv f_0 + a(z/L)^4 - b(z/L)^2$ ($a, b > 0$). We can now directly use results from Ref. [9] to find the following approximated value for the largest Lyapunov exponent:

$$\lambda = \frac{9}{8}\left(1 - \frac{a\Delta}{b^2}\right)^2 \frac{\sqrt{b}(1 + \frac{b}{4a})}{[1 + b(1 + \frac{b}{4a})^2]}, \quad (4)$$

where $b(L_p/L)$ and $a(L_p/L)$ are to be found numerically. The value of λ obtained through Eq. (4) is approximate; e.g., it vanishes only for $L_p/L < 0.25$, whereas a numerical estimate predicts this ratio as 0.4.

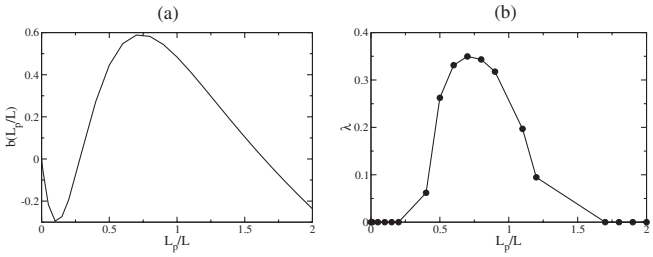

FIG. 4. Plot of (a) b (whose sign determines whether the effective potential is a single or a double well) and (b) λ, as a function of L_p/L for $L = 100a$ and $\Delta = 0.1$, using Eq. (6). (Δ was not fixed by the fluctuation-dissipation theorem, as the system may be out of equilibrium.)

Figure 4 compares the analytical approximation and numerical estimate for the Lyapunov exponent of a grafted polymer. The figure shows an increasing λ with stiffness, a result reminiscent of our simulation. Interestingly the semianalytical treatment also predicts a vanishing λ for large L_p/L. Our analysis highlights the physical origin of the onset of chaotic signatures in grafted semiflexible polymers of intermediate stiffness. As shown in Ref. [16] and as is apparent from Eq. (1) and its approximation, in 2D the distribution probability of the tip position of a grafted semiflexible polymer is bimodal for intermediate stiffness. Hence, the effective free energy governing the tip dynamics (in the close-to-equilibrium regime) is perhaps the simplest paradigm leading to chaotic motion (in the weak damping and deterministic limit, this is the well known Duffing oscillator [14]). Our simulations are in 3D and include pinned as well as grafted boundary conditions, but it is reasonable to postulate that the aperiodic dynamics we observe is qualitatively given by the same physics leading to chaos in the above calculation.

Is the crossover from limit cycle to aperiodic dynamics observable with a state-of-the-art single molecule experiment ? To this end, we propose a controlled force experiment. The force needs to cycle between $-A$ and A, with a frequency increased up to a value $>\tau_r^{-1}$. An AFM force clamp needs $\sim$ms feedback to work, while it can provide forces up to nN at a resolution of 5–10 pN, thereby limiting its applicability to the low force regime [17] (a laser tweezer would provide more stringent constraints but offer a resolution up to $\sim$0.1 pN). τ_r can be accurately estimated via the modified Rouse theory reported in Ref. [18] [Eq. (5) of that work]. For a short dsDNA [as in Fig. 3(d)], an actin fiber ($L \sim 2$ μm, $L_p \sim 17$ μm, $a \sim 5$ nm), and an insulin amyloid fiber ($L \sim 10$ μm, $L_p \sim 7$ μm, $a \sim 5$ nm [19]), in an aqueous solution, $\tau_r \sim 0.2$ ms, 1 s, and 10 s, respectively. Additional simulations suggest that $A \sim$ tens of pN suffices to enter the aperiodic regime in all cases. Therefore, we suggest that our predictions may be testable with actin or insulin fibers in an AFM force clamp (possibly the insulin fiber experiment can be done using laser tweezers).

In conclusion, we have studied the dynamics of a semiflexible polymer grafted or pinned at its ends and subject to a periodic forcing acting on one of its beads. The time series of the process retain strong signatures of nonequilibrium effects. In particular, we observe a crossover from a limit cycle behavior, which reflects the hysteresis inherent to the process, to an aperiodic behavior. A semianalytical approximation shows that for 2D grafted polymers this aperiodic regime has some chaotic signatures as the largest Lyapunov exponent of its ''equivalent'' (in the sense of [9]) deterministic system is positive. This ''chaotic'' signature in the dynamics, at least in part, originates from nontrivial features in the tip distribution probabilities. We hope our studies will stimulate experiments to test the existence of this crossover in the kinetics of a single polymer.

We thank O. E. Akman for useful discussions. A. K. C. acknowledges support from the Marie Curie Foundation.

[1] C. Bustamante, J. C. Macosko, and G. J. L. Wuite, Nat. Rev. Mol. Cell Biol. **1**, 130 (2000); U. Bockelmann, Curr. Opin. Struct. Biol. **14**, 368 (2004); D. E. Smith, H. P. Babcock, and S. Chu, Science **283**, 1724 (1999).
[2] J. F. Marko and E. D. Siggia, Macromolecules **28**, 8759 (1995).
[3] B. Alberts *et al.*, *Molecular Biology of the Cell* (Garland Science, New York, 2003), 4th ed.
[4] S. M. Bhattacharjee and F. Seno, J. Phys. A **36**, L181 (2003); R. Kapri, S. M. Bhattacharjee, and F. Seno, Phys. Rev. Lett. **93**, 248102 (2004).
[5] P. R. Cook, Science **284**, 1790 (1999).
[6] G. Altan-Bonnet, A. Libchaber, and O. Krichevsky, Phys. Rev. Lett. **90**, 138101 (2003); R. Shusterman *et al.*, Phys. Rev. Lett. **92**, 048303 (2004); A. Meller, L. Nivon, and D. Branton, Phys. Rev. Lett. **86**, 3435 (2001); S. E. Henrickson *et al.*, Phys. Rev. Lett. **85**, 3057 (2000); K. Pant, R. L. Karpel, and M. C. Williams, J. Mol. Biol. **327**, 571 (2003).
[7] A. V. Chechkin *et al.*, Phys. Rev. E **67**, 010102(R) (2003); T. Ambjornsson and R. Metzler, Phys. Rev. E **72**, 030901(R) (2005).
[8] M. Doi and S. F. Edwards, *The Theory of Polymer Dynamics* (Clarendon, Oxford, 1988).
[9] S. Datta and J. K. Bhattacharjee, J. Phys. A **34**, L603 (2001).
[10] A. Baumgartner and K. Binder, J. Chem. Phys. **71**, 2541 (1979).
[11] M. Muthukumar, Phys. Rev. Lett. **86**, 3188 (2001).
[12] D. Marenduzzo *et al.*, Phys. Rev. Lett. **88**, 028102 (2001); N. J. Burroughs and D. Marenduzzo, J. Chem. Phys. **123**, 174908 (2005).
[13] V. V. Rybenkov, N. R. Cozzarelli, and A. V. Vologodski, Proc. Natl. Acad. Sci. U.S.A. **90**, 5307 (1993).
[14] S. H. Strogatz, *Nonlinear Dynamics and Chaos* (Addison-Wesley, Reading, MA, 1995).
[15] A. Malevanets and R. Kapral, J. Chem. Phys. **110**, 8605 (1999); I. Ali, D. Marenduzzo, and J. M. Yeomans, Phys. Rev. Lett. **96**, 208102 (2006).
[16] G. Lattanzi, T. Munk, and E. Frey, Phys. Rev. E **69**, 021801 (2004); P. Benetatos, T. Munk, and E. Frey, Phys. Rev. E **72**, 030801(R) (2005).
[17] M. Schlierf, H. Li, and J. M. Fernandez, Proc. Natl. Acad. Sci. U.S.A. **101**, 7299 (2004); M. C. Williams and I. Rouzina, Curr. Opin. Struct. Biol. **12**, 330 (2002).
[18] J.-C. Meiners and S. R. Quake, Phys. Rev. Lett. **84**, 5014 (2000).
[19] J. F. Smith *et al.*, Proc. Natl. Acad. Sci. U.S.A. **103**, 15 806 (2006).
[20] One MCS may be mapped to $\sim$2 ns in a waterlike solvent.